

Search for point sources of ultra-high energy photons with the Telescope Array surface detector

R.U. Abbasi¹, M. Abe², T. Abu-Zayyad¹, M. Allen¹, R. Azuma³, E. Barcikowski¹, J.W. Belz¹, D.R. Bergman¹, S.A. Blake¹, R. Cady¹, B.G. Cheon⁴, J. Chiba⁵, M. Chikawa⁶, A. di Matteo⁷, T. Fujii^{8,9}, K. Fujita¹⁰, R. Fujiwara¹⁰, M. Fukushima^{11,12}, G. Furlich¹, W. Hanlon¹, M. Hayashi¹³, Y. Hayashi¹⁰, N. Hayashida¹⁴, K. Hibino¹⁴, K. Honda¹⁵, D. Ikeda¹¹, N. Inoue², T. Ishii¹⁵, R. Ishimori³, H. Ito¹⁶, D. Ivanov¹, H.M. Jeong¹⁷, S. Jeong¹⁷, C.C.H. Jui¹, K. Kadota¹⁸, F. Kakimoto³, O. Kalashev¹⁹, K. Kasahara²⁰, H. Kawai²¹, S. Kawakami¹⁰, S. Kawana², K. Kawata¹¹, E. Kido¹¹, H.B. Kim⁴, J.H. Kim¹, J.H. Kim²², S. Kishigami¹⁰, S. Kitamura³, Y. Kitamura³, V. Kuzmin^{19*}, M. Kuznetsov¹⁹, Y.J. Kwon²³, K.H. Lee¹⁷, B. Lubsandorzhiev¹⁹, J.P. Lundquist¹, K. Machida¹⁵, K. Martens¹², T. Matsuyama¹⁰, J.N. Matthews¹, R. Mayta¹⁰, M. Minamino¹⁰, K. Mukai¹⁵, I. Myers¹, K. Nagasawa², S. Nagataki¹⁶, K. Nakai¹⁰, R. Nakamura²⁴, T. Nakamura²⁵, T. Nonaka¹¹, H. Oda¹⁰, S. Ogio^{10,26}, J. Ogura³, M. Ohnishi¹¹, H. Ohoka¹¹, T. Okuda²⁷, Y. Omura¹⁰, M. Ono¹⁶, R. Onogi¹⁰, A. Oshima¹⁰, S. Ozawa²⁰, I.H. Park¹⁷, M.S. Pshirkov^{19,28}, J. Remington¹, D.C. Rodriguez¹, G. Rubtsov¹⁹, D. Ryu²², H. Sagawa¹¹, R. Sahara¹⁰, K. Saito¹¹, Y. Saito²⁴, N. Sakaki¹¹, T. Sako¹¹, N. Sakurai¹⁰, L.M. Scott²⁹, T. Seki²⁴, K. Sekino¹¹, P.D. Shah¹, F. Shibata¹⁵, T. Shibata¹¹, H. Shimodaira¹¹, B.K. Shin¹⁰, H.S. Shin¹¹, J.D. Smith¹, P. Sokolsky¹, B.T. Stokes¹, S.R. Stratton^{1,29}, T.A. Stroman¹, T. Suzawa², Y. Takagi¹⁰, Y. Takahashi¹⁰, M. Takamura⁵, M. Takeda¹¹, R. Takeishi¹⁷, A. Taketa³⁰, M. Takita¹¹, Y. Tameda³¹, H. Tanaka¹⁰, K. Tanaka³², M. Tanaka³³, Y. Tanoue¹⁰, S.B. Thomas¹, G.B. Thomson¹, P. Tinyakov^{7,19}, I. Tkachev¹⁹, H. Tokuno³, T. Tomida²⁴, S. Troitsky¹⁹, Y. Tsunesada^{10,26}, K. Tsutsumi³, Y. Uchihori³⁴, S. Udo¹⁴, F. Urban³⁵, T. Wong¹, K. Yada¹¹, M. Yamamoto²⁴, H. Yamaoka³³, K. Yamazaki¹⁴, J. Yang³⁶, K. Yashiro⁵, H. Yoshii³⁷, Y. Zhezher¹⁹, and Z. Zundel¹

¹ High Energy Astrophysics Institute and Department of Physics and Astronomy, University of Utah, Salt Lake City, Utah, USA

² The Graduate School of Science and Engineering, Saitama University, Saitama, Saitama, Japan

³ Graduate School of Science and Engineering, Tokyo Institute of Technology, Meguro, Tokyo, Japan

⁴ Department of Physics and The Research Institute of Natural Science, Hanyang University, Seongdong-gu, Seoul, Korea

⁵ Department of Physics, Tokyo University of Science, Noda, Chiba, Japan

⁶ Department of Physics, Kindai University, Higashi Osaka, Osaka, Japan

⁷ Service de Physique Theorique, Universite Libre de Bruxelles, Brussels, Belgium

⁸ Hakubi Center for Advanced Research, Kyoto University, Sakyo-ku, Kyoto, Japan

⁹ Graduate School of Science, Kyoto University, Sakyo-ku, Kyoto, Japan

¹⁰ Graduate School of Science, Osaka City University, Osaka, Osaka, Japan

¹¹ Institute for Cosmic Ray Research, University of Tokyo, Kashiwa, Chiba, Japan

¹² Kavli Institute for the Physics and Mathematics of the Universe (WPI), Todai Institutes for Advanced Study, University of Tokyo, Kashiwa, Chiba, Japan

¹³ Information Engineering Graduate School of Science and Technology, Shinshu University, Nagano, Nagano, Japan

¹⁴ Faculty of Engineering, Kanagawa University, Yokohama, Kanagawa, Japan

¹⁵ Interdisciplinary Graduate School of Medicine and Engineering, University of Yamanashi, Kofu, Yamanashi, Japan

¹⁶ Astrophysical Big Bang Laboratory, RIKEN, Wako, Saitama, Japan

¹⁷ Department of Physics, Sungkyunkwan University, Jang-an-gu, Suwon, Korea

¹⁸ Department of Physics, Tokyo City University, Setagaya-ku, Tokyo, Japan

¹⁹ Institute for Nuclear Research of the Russian Academy of Sciences, Moscow, Russia

²⁰ Advanced Research Institute for Science and Engineering, Waseda University, Shinjuku-ku, Tokyo, Japan

²¹ Department of Physics, Chiba University, Chiba, Chiba, Japan

²² Department of Physics, School of Natural Sciences, Ulsan National Institute of Science and Technology, UNIST-gil, Ulsan, Korea

²³ Department of Physics, Yonsei University, Seodaemun-gu, Seoul, Korea

²⁴ Academic Assembly School of Science and Technology Institute of Engineering, Shinshu University, Nagano, Nagano, Japan

²⁵ Faculty of Science, Kochi University, Kochi, Kochi, Japan

²⁶ Nambu Yoichiro Institute of Theoretical and Experimental Physics, Osaka City University, Osaka, Osaka, Japan

²⁷ Department of Physical Sciences, Ritsumeikan University, Kusatsu, Shiga, Japan

²⁸ Sternberg Astronomical Institute, Moscow M.V. Lomonosov State University, Moscow, Russia

²⁹ Department of Physics and Astronomy, Rutgers University - The State University of New Jersey, Piscataway, New Jersey, USA

³⁰ Earthquake Research Institute, University of Tokyo, Bunkyo-ku, Tokyo, Japan

³¹ Department of Engineering Science, Faculty of Engineering, Osaka Electro-Communication University, Neyagawa-shi, Osaka, Japan

³² Graduate School of Information Sciences, Hiroshima City University, Hiroshima, Hiroshima, Japan

³³ Institute of Particle and Nuclear Studies, KEK, Tsukuba, Ibaraki, Japan

³⁴ National Institute of Radiological Science, Chiba, Chiba, Japan

* Deceased

** Corresponding author, mkuzn@inr.ac.ru

³⁵ *CEICO, Institute of Physics, Czech Academy of Sciences, Prague, Czech Republic*

³⁶ *Department of Physics and Institute for the Early Universe, Ewha Womans University, Seodaaemun-gu, Seoul, Korea*

³⁷ *Department of Physics, Ehime University, Matsuyama, Ehime, Japan*

Abstract

The surface detector (SD) of the Telescope Array (TA) experiment allows one to indirectly detect photons with energies of order 10^{18} eV and higher and to separate photons from the cosmic-ray background. In this paper we present the results of a blind search for point sources of ultra-high energy (UHE) photons in the Northern sky using the TA SD data. The photon-induced extensive air showers (EAS) are separated from the hadron-induced EAS background by means of a multivariate classifier based upon 16 parameters that characterize the air shower events. No significant evidence for the photon point sources is found. The upper limits are set on the flux of photons from each particular direction in the sky within the TA field of view, according to the experiment's angular resolution for photons. Average 95% C.L. upper limits for the point-source flux of photons with energies greater than 10^{18} , $10^{18.5}$, 10^{19} , $10^{19.5}$ and 10^{20} eV are 0.094, 0.029, 0.010, 0.0073 and $0.0058 \text{ km}^{-2}\text{yr}^{-1}$ respectively. For the energies higher than $10^{18.5}$ eV, the photon point-source limits are set for the first time. Numerical results for each given direction in each energy range are provided as a supplement to this paper.

Keywords: ultra-high energy gamma rays, Telescope Array experiment

I. INTRODUCTION

Ultra-high energy photons are an important tool for studying the high-energy Universe. A plausible source of EeV-energy photons is provided by ultra-high energy cosmic rays (UHECR) undergoing the Greisen-Zatsepin-Kuzmin process [1, 2] or pair production process [3] on a cosmic background radiation. In this context, the EeV photons can be a probe of UHECR mass composition as well as of the distribution of their sources [4, 5]. At the same time, the possible flux of photons produced by UHE protons in the vicinity of their sources by pion photoproduction or inelastic nuclear collisions would be noticeable only for relatively near sources, as the UHE photons attenuation length is smaller than that of UHE protons (see e.g. Ref. [6] for a review). There also exists a class of so-called top-down models of UHECR generation that efficiently produce the UHE photons, for instance by the decay of heavy dark-matter particles [7, 8] or by the radiation from cosmic strings [9]. The search for the UHE photons was shown to be the most sensitive method of indirect detection of heavy dark matter [10–14]. Another fundamental physics scenario that could be tested with UHE photons [15] is the photon mixing with the axion-like particles [16] that could be responsible for the correlation of UHECR events with BL Lac type objects observed by the HiRes experiment [17, 18]. In most of these scenarios, clustering of photon arrival directions rather than diffuse distribution is expected, therefore point-source searches can be a suitable test for them. Finally, the UHE photons could also be used as a probe for the models of Lorentz-invariance violation [19–23].

Telescope Array [24, 25] is the largest cosmic-ray experiment in the Northern Hemisphere. It is located at 39.3° N, 112.9° W in Utah, USA. The observatory includes a surface detector array (SD) and 38 fluorescence

telescopes grouped into three stations. The SD consists of 507 stations that contain plastic scintillators each of 3 m^2 area (SD stations). The stations are placed in the square grid with the 1.2 km spacing and covers the area of $\sim 700 \text{ km}^2$. The TA SD is capable of detecting EAS in the atmosphere caused by cosmic particles of EeV and higher energies. The TA SD operates since May 2008.

A hadron-induced extensive air shower (EAS) significantly differs from an EAS induced by a photon: the depth of the shower maximum X_{max} for a photon shower is larger, a photon shower contains less muons and as a consequence has more curved front (see Ref. [26] for the review). The TA SD stations are sensitive to both muon and electromagnetic component of the shower and therefore may be triggered by both hadron-induced and photon-induced EAS.

In the present study, we use 9 years of TA SD data for a blind search for point sources of UHE photons. We utilize the statistics of the SD data, which benefits from high duty cycle. The full Monte-Carlo (MC) simulation of proton-induced and photon-induced EAS events allows us to perform the photon search up to the highest accessible energies, $E \gtrsim 10^{20}$ eV. As the main tool for the present photon search we use a multivariate analysis based on a number of the SD parameters that make possible to distinguish between photon and hadron primaries.

While searches for diffuse UHE photons were performed by several EAS experiments, including AGASA, Yakutsk and Pierre Auger experiments [27–36], as well as by TA [37, 38], the search for point sources of photons at ultra-high energies has been made only by the Pierre Auger Observatory [39, 40]. The latter searches were based on the hybrid data and were limited to $10^{17.3} < E < 10^{18.5}$ eV energy range. In the present paper we use the TA SD data alone. We perform the searches in five energy ranges, namely $E > 10^{18}$, $E > 10^{18.5}$, $E > 10^{19}$, $E > 10^{19.5}$ and $E > 10^{20}$ eV. As a result we find no significant evidence of photon point sources in all energy

ranges and set the point-source flux upper limits from each direction in TA field of view. The search for unspecified neutral particles was also previously performed by the Telescope Array [41]. The limit on the neutral particles point-source flux obtained in that work is close to the present photon point-source flux limits.

II. TA SD DATA AND RECONSTRUCTION

A. Data set and Monte-Carlo

The data and Monte-Carlo sets used in this study are the same as in the recent TA search for diffuse photons [38]. We use the TA SD data set obtained in 9 years of observation, from May 11, 2008 to May 10, 2017. During this period, the duty cycle of the SD was about 95% [42, 43].

Monte-Carlo simulations used in this study reproduce 9 years of TA SD observations, as it was shown in Ref. [43]. We simulate separately showers induced by photon and proton primaries for the signal and background estimation respectively¹⁾, using the CORSIKA code [44]. The high energy nuclear interactions are simulated with QGSJET-II-03 model [45], the low energy nuclear reactions with FLUKA package [46] and the electromagnetic shower component with EGS4 model [47]. The usage of the PRESHOWER package [48] that takes into account the splitting of the UHE photon primaries into the Earth's magnetic field allows us to correctly simulate photon-induced EAS up to the 100 EeV primary energy and higher. The thinning and dethinning procedures with parameters described in Ref. [49] are used to reduce the calculation time.

We simulated 2100 CORSIKA showers for photon primaries and 9800 for proton primaries in $10^{17.5} - 10^{20.5}$ eV primary energy range. The power spectrum for CORSIKA photon events is set to E^{-1} . The showers from the photon and the proton libraries are processed by the code simulating the real time calibration SD response by means of GEANT4 package [50]. Each CORSIKA event is thrown to the random locations within the SD area multiple times. For photons, these procedures also include reweighting of the events to the E^{-2} differential spectrum, which is assumed for primary photons in this work. As a result, a set of 57 million photon events with E^{-2} spectrum was obtained. The proton Monte-Carlo set used in this study contains approximately 210 million of events. Details of proton Monte-Carlo simulations are described in Refs. [42, 43, 51]. The format of the Monte-Carlo events is the same as the one used for real events, therefore both data and Monte-Carlo are processed by one and the same reconstruction procedure [51] described below.

B. Reconstruction

In this paper, the same procedure to reconstruct shower parameters is used as in the previous TA photon search works [37, 38]. Each either real or simulated event, is reconstructed by a joint fit of the shower-front geometry and the lateral distribution function (LDF) that allows us to determine the shower parameters, including the arrival direction, the core location, the signal density at the fixed distance from the core and the shower front curvature parameter (see Ref. [37] for details).

We apply the following set of the quality cuts for both MC and data events:

1. Zenith angle cut: $0^\circ < \theta < 60^\circ$.
2. The number of stations triggered is 7 or more.
3. The shower core is inside the array boundary with the distance to the boundary larger than 1200 m.
4. Joint fit quality cut: $\chi^2/\text{d.o.f.} < 5$.

We also use an additional cut to eliminate the events induced by lightnings. It was previously studied by the TA collaboration that lightning strikes could cause events mimicking EAS events, the so-called terrestrial gamma-ray flashes (TGF) [52, 53]. Moreover, as the lightning events are expected to be electromagnetic, they resemble photon-induced showers. Therefore, the rejection of these events is crucial for photon search. To make this rejection, we use the Vaisala lightning database from the U.S. National Lightning Detection Network (NLDN) [54–56]. From this database we extract the list of the NLDN lightning events detected within a 15-mile radius circle from the Central Laser Facility of the TA, that contains all the TA SD stations, in a time range from 2008-05-11 to 2017-05-10. The list contains 31622 events grouped in time in such a way that a total of 910 astronomical hours contain one or more lightnings. To clean up all possible lightning-induced events from the data set we remove all the events that occur within 10 minutes time intervals before or after the NLDN lightnings. This cut removes the events known to be related to the TGFs reducing the total exposure only by 0.66% and the total number of data events by 0.77%.

The basic observables calculated in the reconstruction procedure together with several additional parameters (see below), are used to distinguish photon and proton events by means of a multivariate analysis. Some of the observables are utilizing the features of the experiment's SD technical design, such as the double-layered scintillators. The detailed description of these technical parameters is given in Ref. [24]. The full list of 16 parameters used in the present photon search is the same as in the TA SD search for diffuse photons [38] and the TA SD composition study [57]. Namely, the parameters are:

1. Zenith angle, θ .
2. Signal density at 800 m from the shower core, S_{800} .

¹⁾ We justify the proton background assumption in the Sec. III A.

3. Linsley front curvature parameter, a obtained from the fit of the shower front with the AGASA-modified Linsley time delay function [37, 58].
4. Area-over-peak (AoP) of the signal at 1200 m [59].
5. AoP slope parameter [60].
6. Number of stations with Level-0 trigger [24] (triggered stations).
7. Number of stations excluded from the fit of the shower front due to large contribution to χ^2 .
8. $\chi^2/d.o.f.$ of the shower front fit.
9. S_b parameter for $b = 3$; S_b is defined as b -th moment of the LDF:

$$S_b = \sum_i \left[S_i \times (r_i/r_0)^b \right], \quad (1)$$

where S_i is the signal of i -th station, r_i is the distance from the shower core to a given station, $r_0 = 1000$ m. The sum is calculated over all triggered non-saturated stations. The S_b is proposed as a composition-sensitive parameter in Ref. [61].

10. S_b parameter for $b = 4.5$.
11. The sum of signals of all triggered stations of the event.
12. An average asymmetry of signal at upper and lower layers of the stations defined as:

$$\mathcal{A} = \frac{\sum_{i,\alpha} |s_{i,\alpha}^{upper} - s_{i,\alpha}^{lower}|}{\sum_{i,\alpha} |s_{i,\alpha}^{upper} + s_{i,\alpha}^{lower}|}, \quad (2)$$

where $s_{i,\alpha}^{upper|lower}$ is the FADC value of upper or lower layer of i -th station at α -th time bin. The sum is calculated over all triggered non-saturated stations over all time bins of the corresponding FADC traces.

13. Total number of peaks of FADC trace summed over upper and lower layers of all triggered stations of the event. To suppress accidental peaks as a result of FADC noise, we define a peak as a time bin with a signal above 0.2 Vertical equivalent muons (VEM) which is higher than a signal of the 3 preceding and 3 consequent time bins.
14. Number of peaks for the station with the largest signal.
15. Total number of peaks present in the upper layer and not in the lower one, summed over all triggered stations of the event.

16. Total number of peaks present in the lower layer and not in the upper one, summed over all triggered stations of the event.

For each MC and data event we also define the “photon energy” parameter E_γ which is the expected energy of the primary particle assuming it is a photon. This energy parameter is calculated as the function of the zenith angle and the S_{800} parameter, from the photon MC simulations [37]. For proton MC events, as well as for the majority of data events, the E_γ parameter is not the actual primary energy but merely a parameter needed for the consistent comparison of proton events and possible photon events. It is important to note that for majority of proton-induced events, the reconstructed E_γ parameter is systematically higher than that of photon-induced events of the same primary Monte-Carlo energy. For instance, at ~ 10 EeV Monte-Carlo energy the mean E_γ for protons is $\sim 40\%$ higher than that for photons, if we assume the averaging over zenith angle. Due to this fact the proton background for SD photon search is higher with respect to the hypothetical ideal situation when the energy reconstruction bias is independent of the primary particle type. All the energy values considered in this work is assumed to be E_γ values, unless the other meaning is specified.

The reconstructed values of shower zenith angle, θ_{rec} , for photon primaries are systematically underestimated. The possible reason for this is the azimuthal asymmetry of the shower front, that originates from the fact that the shower arrives younger to the front-side stations and older to the back-side ones. The reconstruction bias is defined as a deviation of the event θ_{rec} from a real Monte-Carlo zenith angle of this event, θ_{true} . The average values of this bias for various energies E_γ are given in Table I. In this study we correct both proton and photon Monte-Carlo events and data events by these average bias values. This correction allows us to restore arrival directions of possible photon-induced events more accurately, while not affecting the background of hadron-induced events, which is known to be highly isotropic [62]. Another crucial parameter for the point-source search is the angular resolution of the experiment. It is defined as a 0.68 percentile of a distribution of Monte-Carlo events over opening angle between event reconstructed arrival direction and real Monte-Carlo arrival direction. The angular resolution of TA SD for proton primaries at “proton energy”, $E_p = 10^{19}$ eV, was estimated to be 1.5° [63]. As it was mentioned above, in the present study we use the reconstruction of Ref. [37] for both data and Monte-Carlo events. Using the photon Monte-Carlo set, after applying the zenith-angle bias correction described above, we estimate the angular resolution for photon primaries at various energies E_γ . The results are shown in Table I.

E_γ , eV	$\langle\theta_{\text{rec.}} - \theta_{\text{true}}\rangle$	ang. resolution
$> 10^{18.0}$	-2.25°	3.00°
$> 10^{18.5}$	-2.24°	2.92°
$> 10^{19.0}$	-2.16°	2.64°
$> 10^{19.5}$	-2.06°	2.21°
$> 10^{20.0}$	-1.72°	2.06°

TABLE I. Bias in the reconstruction of the zenith angle and angular resolution for the photon primaries at various energies.

III. ANALYSIS

A. Multivariate analysis

The analysis method used in this study to distinguish between photon and proton events is a boosted decision tree (BDT) classifier built with the 16 observable parameters listed in the previous section. As an implementation of this method, we use the AdaBoost algorithm [64] from the TMVA package [65] for ROOT [66], in the same way as in the recent TA studies [38, 57].

The BDT is trained to separate proton MC events from photon MC events. Both proton and photon MC sets are split into three parts with equal amount of events in each: one for training the classifier, the second one for testing the classifier and the last one for the calculation of proton background and photon effective exposure, respectively. We train the classifier separately in five photon energy ranges: $E_\gamma > 10^{18}$ eV, $E_\gamma > 10^{18.5}$ eV, $E_\gamma > 10^{19}$ eV, $E_\gamma > 10^{19.5}$ eV and $E_\gamma > 10^{20}$ eV. As a result of the BDT procedure, the single multivariate analysis (MVA) parameter ξ is assigned to each MC and data event. ξ is defined to take values in the range $-1 < \xi < 1$, where proton-induced events tend to have negative ξ values, and photon-induced events — positive ξ values. The resulting ξ distributions of the MC events from the testing sets and the data events for the all considered energy ranges are shown in Fig. 1. The obtained ξ distributions are available for the further one dimensional analysis.

From Fig. 1, which shows the distributions of data and Monte-Carlo irrespective of the direction in the sky, one can observe no deviation from the proton distribution in the expected photon signal region. However, possible excesses in one or several separate directions in the sky could be overlooked if we analyze the all-sky averaged ξ distribution. Hereafter we discuss methods to set photon-flux upper limit and to search for photon excesses from separate directions in the sky and then present respective results.

It is important to note that at primary energies of order EeV and higher there is a potential systematic uncertainty in the estimation of the hadron background for the photon signal. The bulk of the events are induced by protons and/or nuclei, but their mass composition is not known precisely [57, 67, 68]. We have examined ξ distributions of the iron nucleus-induced events and found that

in average the iron-induced events are less "photon-like" than proton-induced events. The results of TA work [57], where the similar BDT-classifier was used, implies that a mixed nuclei ξ distribution would also deviate from the photon ξ distribution stronger than the proton ξ distribution. Therefore, we assume that the choice of the proton background for the photon search is conservative.

B. Photon-flux upper limit

In general, the flux upper limit for the particular type of primaries is defined as:

$$F_{\text{UL}} = \frac{\mu_{\text{FC}}(N_{\text{bg}}, N_{\text{obs}})}{A_{\text{eff}}} \quad (3)$$

where N_{obs} is the number of detected events of a given type in a given energy range, N_{bg} is the estimated number of background events in the same energy range, μ_{FC} is the upper bound of the respective Poisson mean for the given confidence level, defined according to Ref. [69], and A_{eff} is the effective exposure of the experiment for the given type of primaries in the same energy range.

In the present upper-limit calculation we assume the "null hypothesis", i.e. that there is actually no photons and any excess counts from the expected background, $N_{\text{obs}} - N_{\text{bg}}$, is considered as a fluctuation of background, while the value of N_{bg} itself in Eq. 3 is set to zero. This assumption is conservative since for the fixed N_{obs} the upper-limit value is higher for a lower value of N_{bg} . According the discussion in the end of previous Section we assume the background to be pure protons, $N_{\text{obs}} = N_{\text{p}}$.

The separation between photon and proton primaries is defined by a cut on MVA-variable ξ . The cut is set at some value ξ_0 so that any proton with $\xi > \xi_0$ is considering as a photon candidate and any photon with $\xi > \xi_0$ is contributing to the effective exposure. To find the minimum value of F_{UL}^γ as a function of ξ_0 we optimize the cut position assuming the null hypothesis: $N_{\text{obs}} = N_{\text{p}}(\xi > \xi_0)$; $N_{\text{bg}} = 0$, where $N_{\text{p}}(\xi > \xi_0)$ is the number of protons passing the ξ -cut. As one can see from Fig. 1, the number of MC photon events passing the ξ -cut is decreasing with the growth of ξ_0 leading to the respective decrease of the exposure A_{eff}^γ , also the number of photon candidates, $N_{\text{obs}} = N_{\text{p}}(\xi > \xi_0)$, is decreasing, but $N_{\text{obs}} = 0$ yields a constant non-zero value of μ_{FC} .

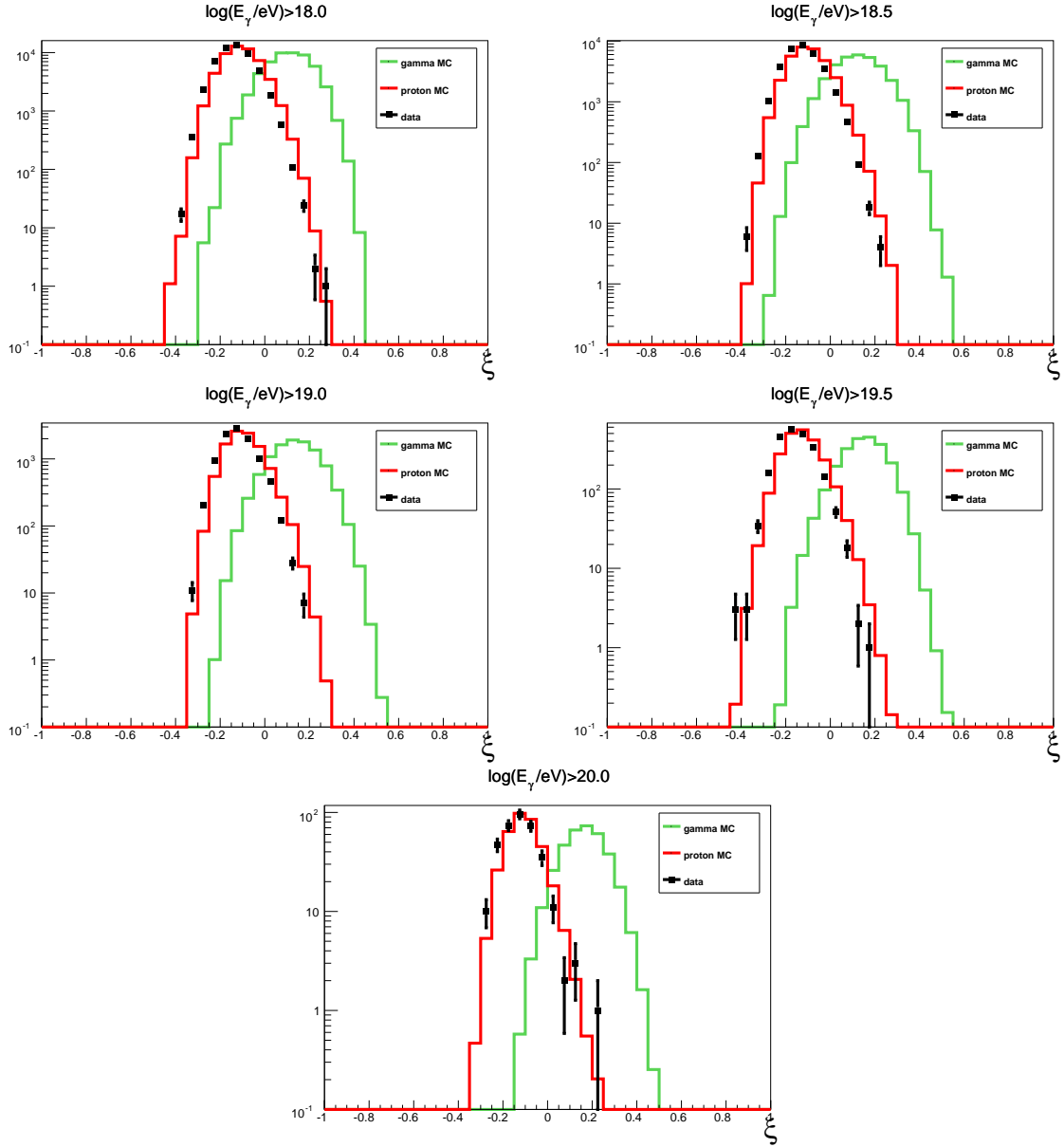


FIG. 1. The distributions of the photon and proton Monte-Carlo and data events over the ξ parameter for the five energy ranges (solid red — protons, solid green — photons, black dots — data).

This implies that there indeed should be a non-trivial minimum value of F_{UL}^γ as a function of ξ_0 .

For the ξ -cut optimization we use the proton Monte-Carlo set normalized to the size of the data set and the photon Monte-Carlo set, the latter is used for the calculation of the photon effective exposure A_{eff}^γ . It is important to note that the optimization procedure tends to place ξ_0 at the right edge of the proton distribution in Fig. 1, therefore the number of candidates N_{obs} and the upper-limit value F_{UL} are subject to fluctuations. These fluctuations become apparent when one considers upper limits for particular directions in the sky with small number of events.

Up to this moment the procedures of upper-limit calculation and cut optimization were similar to those used to search for diffuse photons [38]. The difference of the analysis procedure used here from that of Ref. [38] is in the usage of the separate event sets for different directions in the sky. The ξ -cut is also optimized separately for every direction studied. We pixelize the sky in equatorial coordinates $\{\alpha, \delta\}$ using the HEALPix package [70] into 12288 pixels ($N_{\text{side}} = 32$). For the pixel “i” with the center $\{\alpha_i, \delta_i\}$ the corresponding data set contains events located inside a spherical cap region around the pixel center within an angular distance that equals to the experiment’s angular resolution at the respective energy

(see Tab. I)¹⁾.

The effective exposure of the experiment to photons at the pixel “i” is given by:

$$A_{\text{eff}}^i = S \cdot T \cdot \frac{\overline{\cos \theta_i} N_{MC,\gamma}^i(\xi > \xi_0)}{N_{MC,\gamma}^i} \quad (4)$$

where S is the area of the experiment, T is the period of observation, θ_i is the zenith angle at which the pixel “i” is seen by the experiment, $N_{MC,\gamma}^i$ is the total number of photon events simulated in the respective pixel and $N_{MC,\gamma}^i(\xi > \xi_0)$ is the number of these events that pass the ξ -cut. The same pixel in equatorial coordinates is seen by the experiment at different θ depending on time, therefore the diurnal mean value $\overline{\cos \theta}$ is used. It is given by the expression[71]:

$$\overline{\cos \theta} = \cos \lambda_0 \cos \delta \sin \alpha_m + \alpha_m \sin \lambda_0 \sin \delta, \quad (5)$$

where δ is the declination, λ_0 is the geographical latitude of the experiment, θ_{max} is the maximum zenith angle of the events considered in the particular analysis and α_m is given by the expression

$$\alpha_m = \begin{cases} 0 & ; \zeta > 1, \\ \pi & ; \zeta < -1, \\ \arccos \zeta & ; -1 < \zeta < 1; \end{cases} \quad (6)$$

where

$$\zeta = \frac{(\cos \theta_{\text{max}} - \sin \lambda_0 \sin \delta)}{\cos \lambda_0 \cos \delta}. \quad (7)$$

The “effective” part of the exposure, $\frac{N_{MC,\gamma}^i(\xi > \xi_0)}{N_{MC,\gamma}^i}$, is calculated using the photon Monte-Carlo. To have enough statistics for this calculation, one needs to generate separate Monte-Carlo sets for each sky-map pixel. However, it is technically unreasonable, since the exposure depends only on declination of the given pixel. We use the following method to increase the Monte-Carlo statistics in each pixel: ξ_0 is optimized over the events belonging to the whole constant-declination band whose width is twice the angular resolution centered in the given pixel.

This method resembles the so-called “scrambling technique” [72], which was used for instance in the Pierre Auger Observatory search for photon point sources [39]. The additional advantage of the used method is the preservation of relatively large effective statistics of the Monte-Carlo events in each pixel, including the variety

over ξ -parameter. We have found that in this case, fluctuations of the ξ_0 position between adjacent pixels are smaller, compared to the standard scrambling technique. It is reasonable to smooth these fluctuations even further by making a least-squares fit of a ξ_0 position as a function of declination with a smooth function, for which we use a second-order polynomial. As it has been mentioned before, the flux upper limit remains conservative after this operation. The examples of ξ_0 as a function of declination and its smooth fitting are shown in Fig. 2²⁾.

As the ξ_0 position for the pixel “i” is fixed, the actual upper-limit value is calculated using the definition (3) with $N_{\text{bg}}^i = 0$ and $N_{\text{obs}}^i = N_{\text{data}}^i(\xi > \xi_0)$, where N_{data}^i is the number of the data events belonging to the respective pixel.

The Telescope Array field of view for the considered zenith angle cut ($0^\circ < \theta < 60^\circ$) spans from -20.7° to 90° in declination. However, the event statistics is low in the constant-declination bands near the edges of this interval. Therefore we reduce the considered sky region to $-15.7^\circ \leq \delta \leq 85^\circ$. It contains 7868 pixels.

C. Results

The photon-flux upper limits at 95% C.L. for each pixel in the Telescope Array field of view and for various photon energies are shown in Fig. 3. The numerical values of these limits are collected in the supplementary material. The values of the limits averaged over all pixels are presented in Table II.

The null hypothesis assumed for the photon upper-limit calculation is not optimal for the photon search. However the rough estimation of the possible photon signal could be made already in this setup. We optimize ξ_0 in each declination band with the same assumptions as in the previous section, and estimate the background in each pixel as the appropriately normalized number of protons that pass the cut: $N_{MC,p}^i(\xi > \xi_0)$. For the photon excess calculation, the assumption of proton background is conservative as it should be higher than any mixed nuclei background, as it was discussed in Sec. III A. The background maps for various photon energies are shown in Fig. 4. The maxima over all pixels pre-trial photon candidate excesses over the proton background are presented in the Table II along with the average over all pixels values of the proton background. The highest pre-trial excess significance, 3.43σ ($N_{\text{bg}} = 0.036$ and $N_{\text{obs}} = 2$), appears in the highest energy bin $E_\gamma > 10^{20}$ eV, at $\{\alpha = 155.3^\circ, \delta = 60.4^\circ\}$ pixel. To make a simple estimation of the post-trial p-value one can use the Bonferroni correction, i.e. to multiply the number of trials by the minimum pre-trial ex-

¹⁾ The distance between any pixel centers is smaller than experiment’s angular resolution at all considered energies, therefore the experiment FOV is overlapped without gaps, but some events in adjacent pixels could be the same.

²⁾ The ξ_0 points for adjacent declination bands are clustered because these bands are overlapping with each other and a part of their MC events is one and the same.

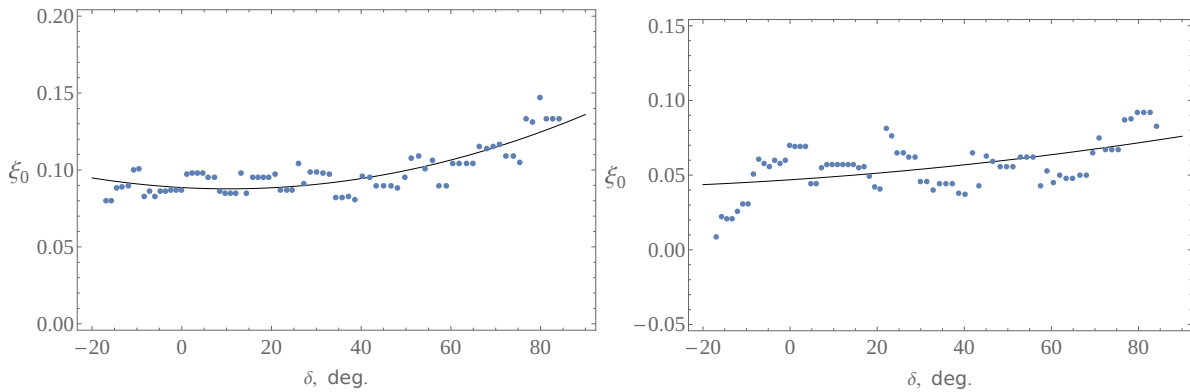


FIG. 2. Examples of ξ_0 position as a function of declination and its smooth fitting for $E_\gamma > 10^{18}$ eV (left panel) and $E_\gamma > 10^{19}$ eV (right panel) photons. Blue points are the cut positions obtained with the optimization of the photon flux-upper limit Eq. (3) in the respective declination bands.

E_γ , eV	$\langle F_\gamma \rangle \leq$, $\text{km}^{-2}\text{yr}^{-1}$	$\langle N_{\text{bg}} \rangle$	max. γ signif. (pre-trial)
$> 10^{18.0}$	0.094	0.49	2.72σ
$> 10^{18.5}$	0.029	0.52	2.71σ
$> 10^{19.0}$	0.010	0.34	2.89σ
$> 10^{19.5}$	7.1×10^{-3}	0.10	2.76σ
$> 10^{20.0}$	5.8×10^{-3}	0.029	3.43σ

TABLE II. Point-source photon-flux upper limits and proton backgrounds averaged over all pixels together with the maximum pre-trial significance of the photon excess over proton background.

cess p-value [73]. In turn, the number of trials could be estimated as the number of non-overlapping pixel-size regions of the map which is several times smaller than the actual number of pixels. The resulting post-trial significances estimated in this way appear to be below 1σ level for all points of the sky at all considered energies. Therefore we concluded that, at the present level of point-source photon search sensitivity, there is no evidence for the photon signal. The actual results for each sky-map pixel at various energies are given in the text files supplemented to this paper. The format of the files is described in the Supplementary section.

The main systematic uncertainties for the photon-flux upper limits are related to the overestimation of the E_γ parameter for hadron-induced events and to the uncertainty of the primary hadron mass-composition. The former uncertainty leads to the overestimation of the hadron background and subsequently to the looser photon-flux upper limit. In the case of the hadron background mass-composition uncertainty, the assumption of the proton composition which we use could also make the photon-flux upper limit only looser, with regard to a mixed nuclei composition case. Therefore the limits set are conservative to the both of these uncertainties.

IV. DISCUSSION AND CONCLUSIONS

The upper limits are set on the fluxes of photons from each particular direction in the sky in the TA field of view, according to the experiment's angular resolution with respect to photons. The only results of the ultra-high energy point-source photon flux upper-limits presented up to now belong to the Pierre Auger experiment [39, 40]. The direct comparison of those results to ours is not proper as the photon energy range of the Auger search, $10^{17.3} < E_\gamma < 10^{18.5}$ eV, does not fully coincide to any of our ranges of search. Regardless of that, the result of Auger for the average point-source photon flux, $\langle F_\gamma \rangle \leq 0.035 \text{ km}^{-2}\text{yr}^{-1}$, is approximately three times stronger than our result for the $E_\gamma > 10^{18}$ eV. The results for the energies larger than $E > 10^{18.5}$ eV are obtained here for the first time.

The point-source photon-flux upper limits derived in the present study can be used to constrain various models of astrophysics and particle physics. One can assume a distribution of photon sources and impose the constraints on their properties using the combination of point-source limits. In principle these constraints could be stronger than those derived with the diffuse photon-flux limits. The models that could be probed with the present photon point-source flux limits include cosmogenic photon generation models as well as top-down models of ultra-

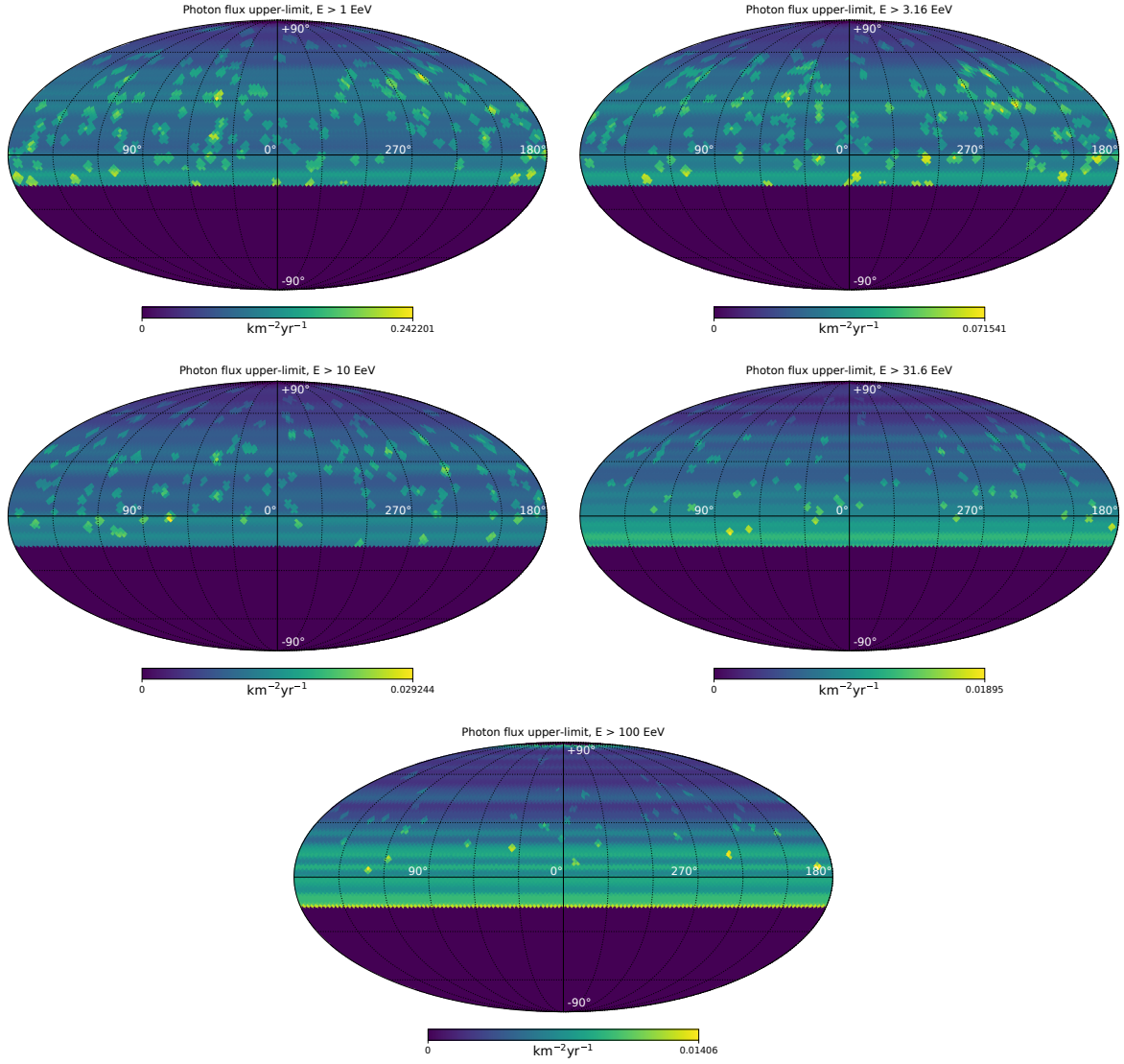


FIG. 3. Maps of point-source photon flux upper limits (95% C.L.) for various photon energies plotted in equatorial coordinates.

high energy photons production such as heavy decaying dark matter.

SUPPLEMENTARY

Photon point-source flux upper limits and photon excess pre-trial significances for all sky-map pixels are summarized in the separate file for each energy bin, named “limit_[$\log(E_\gamma/\text{eV})$].txt”. The file contains several columns with the following data.

Column 1: HEALpix pixel number (RING, started from 0)

Column 2: pixel α , rad.

Column 3: pixel δ , rad.

Column 4: ξ -cut value

Column 5: proton background value

Column 6: number of γ -candidate events

Column 7: F_γ upper limit, $\text{km}^{-2}\text{yr}^{-1}$

Column 8: pre-trial γ excess p-value

Column 9: pre-trial γ excess significance

As it was mentioned in Sec. III C the proton background value is used only for the calculation of photon excess p-value and significance, while the upper limit is calculated in zero background assumption. For pixels with the number of γ -candidates less than p background both p-value and significance are set to zero.

ACKNOWLEDGEMENTS

The Telescope Array experiment is supported by the Japan Society for the Promotion of Science (JSPS) through Grants-in-Aid for Priority Area 431, for Spe-

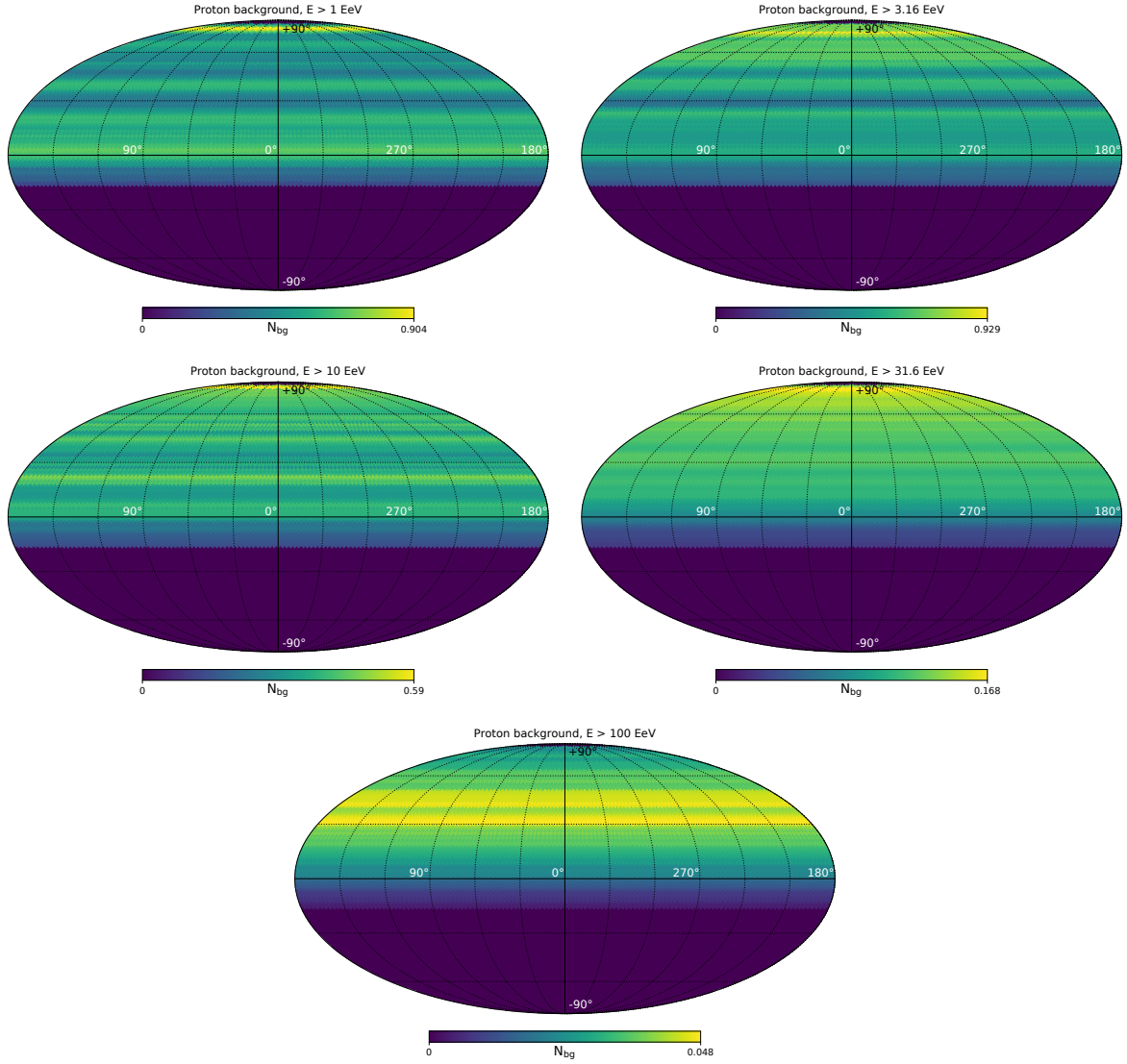


FIG. 4. The distributions of the numbers of proton background events over the sky map for the various photon energies plotted in equatorial coordinates.

cially Promoted Research JP21000002, for Scientific Research (S) JP19104006, for Specially Promoted Research JP15H05693, for Scientific Research (S) JP15H05741, for Science Research (A) JP18H03705 and for Young Scientists (A) JPH26707011; by the joint research program of the Institute for Cosmic Ray Research (ICRR), The University of Tokyo; by the U.S. National Science Foundation awards PHY-0601915, PHY-1404495, PHY-1404502, and PHY-1607727; by the National Research Foundation of Korea (2016R1A2B4014967, 2016R1A5A1013277, 2017K1A4A3015188, 2017R1A2A1A05071429) and Belgian Science Policy under IUAP VII/37 (ULB). The development and application of the multivariate analysis method is supported by the Russian Science Foundation grant No. 17-72-20291 (INR). The foundations of Dr. Ezekiel R. and Edna Wattis Dumke, Willard L. Eccles,

and George S. and Dolores Doré Eccles all helped with generous donations. The State of Utah supported the project through its Economic Development Board, and the University of Utah through the Office of the Vice President for Research. The experimental site became available through the cooperation of the Utah School and Institutional Trust Lands Administration (SITLA), U.S. Bureau of Land Management (BLM), and the U.S. Air Force. We appreciate the assistance of the State of Utah and Fillmore offices of the BLM in crafting the Plan of Development for the site. Patrick Shea assisted the collaboration with valuable advice on a variety of topics. The people and the officials of Millard County, Utah have been a source of steadfast and warm support for our work which we greatly appreciate. We are indebted to the Millard County Road Department for their efforts to main-

tain and clear the roads which get us to our sites. We gratefully acknowledge the contribution from the technical staffs of our home institutions. An allocation of computer time from the Center for High Performance Computing at the University of Utah is gratefully ac-

knowledge. The cluster of the Theoretical Division of INR RAS was used for the numerical part of the work. The lightning data used in this paper was obtained from Vaisala, Inc. We appreciate Vaisala's academic research policy.

-
- [1] Kenneth Greisen. End to the cosmic ray spectrum? *Phys. Rev. Lett.*, 16:748–750, 1966. doi:10.1103/PhysRevLett.16.748.
 - [2] G. T. Zatsepin and V. A. Kuzmin. Upper limit of the spectrum of cosmic rays. *JETP Lett.*, 4:78–80, 1966. [Pisma Zh. Eksp. Teor. Fiz.4,114(1966)].
 - [3] G. R. Blumenthal. Energy loss of high-energy cosmic rays in pair-producing collisions with ambient photons. *Phys. Rev.*, D1:1596–1602, 1970. doi:10.1103/PhysRevD.1.1596.
 - [4] Graciela Gelmini, Oleg E. Kalashev, and Dmitry V. Semikoz. GZK photons as ultra high energy cosmic rays. *J. Exp. Theor. Phys.*, 106:1061–1082, 2008. arXiv:astro-ph/0506128, doi:10.1134/S106377610806006X.
 - [5] Dan Hooper, Andrew M. Taylor, and Subir Sarkar. Cosmogenic photons as a test of ultra-high energy cosmic ray composition. *Astropart. Phys.*, 34:340–343, 2011. arXiv:1007.1306, doi:10.1016/j.astropartphys.2010.09.002.
 - [6] Pijushpani Bhattacharjee and Gunter Sigl. Origin and propagation of extremely high-energy cosmic rays. *Phys. Rept.*, 327:109–247, 2000. arXiv:astro-ph/9811011, doi:10.1016/S0370-1573(99)00101-5.
 - [7] V. Berezhinsky, M. Kachelriess, and A. Vilenkin. Ultrahigh-energy cosmic rays without GZK cutoff. *Phys. Rev. Lett.*, 79:4302–4305, 1997. arXiv:astro-ph/9708217, doi:10.1103/PhysRevLett.79.4302.
 - [8] V. A. Kuzmin and V. A. Rubakov. Ultrahigh-energy cosmic rays: A Window to postinflationary reheating epoch of the universe? *Phys. Atom. Nucl.*, 61:1028, 1998. arXiv:astro-ph/9709187.
 - [9] Veniamin Berezhinsky, Pasquale Blasi, and Alexander Vilenkin. Ultrahigh-energy gamma-rays as signature of topological defects. *Phys. Rev.*, D58:103515, 1998. arXiv:astro-ph/9803271, doi:10.1103/PhysRevD.58.103515.
 - [10] O. K. Kalashev and M. Yu. Kuznetsov. Constraining heavy decaying dark matter with the high energy gamma-ray limits. *Phys. Rev.*, D94(6):063535, 2016. arXiv:1606.07354, doi:10.1103/PhysRevD.94.063535.
 - [11] M. Yu. Kuznetsov. Hadronically decaying heavy dark matter and high-energy neutrino limits. *JETP Lett.*, 105(9):561–567, 2017. arXiv:1611.08684, doi:10.1134/S0021364017090028.
 - [12] O. E. Kalashev and M. Yu. Kuznetsov. Heavy decaying dark matter and large-scale anisotropy of high-energy cosmic rays. *JETP Lett.*, 106(2):73–80, 2017. [Pisma Zh. Eksp. Teor. Fiz.106,no.2,65(2017)]. arXiv:1704.05300, doi:10.1134/S0021364017140016.
 - [13] M. Kachelriess, O. E. Kalashev, and M. Yu. Kuznetsov. Heavy decaying dark matter and IceCube high energy neutrinos. *Phys. Rev.*, D98(8):083016, 2018. arXiv:1805.04500, doi:10.1103/PhysRevD.98.083016.
 - [14] Esteban Alcantara, Luis A. Anchordoqui, and Jorge F. Soriano. Hunting WIMPzilla with the highest-energy cosmic rays. 2019. arXiv:1903.05429.
 - [15] Malcolm Fairbairn, Timur Rashba, and Sergey V. Troitsky. Photon-axion mixing and ultra-high-energy cosmic rays from BL Lac type objects - Shining light through the Universe. *Phys. Rev.*, D84:125019, 2011. arXiv:0901.4085, doi:10.1103/PhysRevD.84.125019.
 - [16] Georg Raffelt and Leo Stodolsky. Mixing of the Photon with Low Mass Particles. *Phys. Rev.*, D37:1237, 1988. doi:10.1103/PhysRevD.37.1237.
 - [17] Dmitry S. Gorbunov, P. G. Tinyakov, I. I. Tkachev, and Sergey V. Troitsky. Testing the correlations between ultra-high-energy cosmic rays and BL Lac type objects with HiRes stereoscopic data. *JETP Lett.*, 80:145–148, 2004. [Pisma Zh. Eksp. Teor. Fiz.80,167(2004)]. arXiv:astro-ph/0406654, doi:10.1134/1.1808838.
 - [18] R. U. Abbasi et al. Search for cross-correlations of ultrahigh-energy cosmic rays with BL Lacertae objects. *Astrophys. J.*, 636:680–684, 2006. arXiv:astro-ph/0507120, doi:10.1086/498142.
 - [19] Sidney R. Coleman and Sheldon L. Glashow. High-energy tests of Lorentz invariance. *Phys. Rev.*, D59:116008, 1999. arXiv:hep-ph/9812418, doi:10.1103/PhysRevD.59.116008.
 - [20] Matteo Galaverni and Gunter Sigl. Lorentz Violation in the Photon Sector and Ultra-High Energy Cosmic Rays. *Phys. Rev. Lett.*, 100:021102, 2008. arXiv:0708.1737, doi:10.1103/PhysRevLett.100.021102.
 - [21] Luca Maccione, Stefano Liberati, and Gunter Sigl. Ultra high energy photons as probes of Lorentz symmetry violations in stringy space-time foam models. *Phys. Rev. Lett.*, 105:021101, 2010. arXiv:1003.5468, doi:10.1103/PhysRevLett.105.021101.
 - [22] Grigory Rubtsov, Petr Satunin, and Sergey Sibiryakov. On calculation of cross sections in Lorentz violating theories. *Phys. Rev.*, D86:085012, 2012. arXiv:1204.5782, doi:10.1103/PhysRevD.86.085012.
 - [23] Grigory Rubtsov, Petr Satunin, and Sergey Sibiryakov. Prospective constraints on Lorentz violation from ultrahigh-energy photon detection. *Phys. Rev.*, D89(12):123011, 2014. arXiv:1312.4368, doi:10.1103/PhysRevD.89.123011.
 - [24] T. Abu-Zayyad et al. The surface detector array of the Telescope Array experiment. *Nucl. Instrum. Meth.*, A689:87–97, 2013. arXiv:1201.4964, doi:10.1016/j.nima.2012.05.079.
 - [25] H. Tokuno et al. New air fluorescence detectors employed in the Telescope Array experiment. *Nucl. Instrum. Meth.*, A676:54–65, 2012. arXiv:1201.0002, doi:10.1016/j.nima.2012.02.044.
 - [26] Markus Risse and Piotr Homola. Search for ultrahigh energy photons using air showers. *Mod. Phys. Lett.*, A22:749–766, 2007. arXiv:astro-ph/0702632, doi:10.

- 1142/S0217732307022864.
- [27] M. Ave, J. A. Hinton, R. A. Vazquez, Alan A. Watson, and E. Zas. New constraints from Haverah Park data on the photon and iron fluxes of UHE cosmic rays. *Phys. Rev. Lett.*, 85:2244–2247, 2000. [arXiv:astro-ph/0007386](#), doi:10.1103/PhysRevLett.85.2244.
 - [28] K. Shinozaki et al. Upper limit on gamma-ray flux above 10^{19} eV estimated by the Akeno Giant Air Shower Array experiment. *Astrophys. J.*, 571:L117–L120, 2002. doi:10.1086/341288.
 - [29] A. V. Glushkov, D. S. Gorbunov, I. T. Makarov, M. I. Pravdin, G. I. Rubtsov, I. E. Sleptsov, and Sergey V. Troitsky. Constraining the fraction of primary gamma rays at ultra-high energies from the muon data of the Yakutsk extensive-air-shower array. *JETP Lett.*, 85:131–135, 2007. [arXiv:astro-ph/0701245](#), doi:10.1134/S0021364007030010.
 - [30] A. V. Glushkov, I. T. Makarov, M. I. Pravdin, I. E. Sleptsov, D. S. Gorbunov, G. I. Rubtsov, and S. V. Troitsky. Constraints on the flux of primary cosmic-ray photons at energies $E > 10^{18}$ eV from Yakutsk muon data. *Phys. Rev.*, D82:041101, 2010. [arXiv:0907.0374](#), doi:10.1103/PhysRevD.82.041101.
 - [31] Markus Risse, P. Homola, R. Engel, D. Gora, D. Heck, J. Pekala, B. Wilczynska, and H. Wilczynski. Upper limit on the photon fraction in highest-energy cosmic rays from AGASA data. *Phys. Rev. Lett.*, 95:171102, 2005. [arXiv:astro-ph/0502418](#), doi:10.1103/PhysRevLett.95.171102.
 - [32] G. I. Rubtsov et al. Upper limit on the ultrahigh-energy photon flux from agasa and yakutsk data. *Phys. Rev.*, D73:063009, 2006. [arXiv:astro-ph/0601449](#), doi:10.1103/PhysRevD.73.063009.
 - [33] J. Abraham et al. An upper limit to the photon fraction in cosmic rays above 10^{19} -eV from the Pierre Auger Observatory. *Astropart. Phys.*, 27:155–168, 2007. [arXiv:astro-ph/0606619](#), doi:10.1016/j.astropartphys.2006.10.004.
 - [34] J. Abraham et al. Upper limit on the cosmic-ray photon flux above 10^{19} eV using the surface detector of the Pierre Auger Observatory. *Astropart. Phys.*, 29:243–256, 2008. [arXiv:0712.1147](#), doi:10.1016/j.astropartphys.2008.01.003.
 - [35] Carla Bleve. Updates on the neutrino and photon limits from the Pierre Auger Observatory. *PoS, ICRC2015:1103*, 2016.
 - [36] Alexander Aab et al. Search for photons with energies above 10^{18} eV using the hybrid detector of the Pierre Auger Observatory. *JCAP*, 1704(04):009, 2017. [arXiv:1612.01517](#), doi:10.1088/1475-7516/2017/04/009.
 - [37] T. Abu-Zayyad et al. Upper limit on the flux of photons with energies above 10^{19} eV using the Telescope Array surface detector. *Phys. Rev.*, D88(11):112005, 2013. [arXiv:1304.5614](#), doi:10.1103/PhysRevD.88.112005.
 - [38] R. U. Abbasi et al. Constraints on the diffuse photon flux with energies above 10^{18} eV using the surface detector of the Telescope Array experiment. 2018. [arXiv:1811.03920](#).
 - [39] Alexander Aab et al. A search for point sources of EeV photons. *Astrophys. J.*, 789(2):160, 2014. [arXiv:1406.2912](#), doi:10.1088/0004-637X/789/2/160.
 - [40] Alexander Aab et al. A targeted search for point sources of EeV photons with the Pierre Auger Observatory. *Astrophys. J.*, 837(2):L25, 2017. [arXiv:1612.04155](#), doi:10.3847/2041-8213/aa61a5.
 - [41] R. U. Abbasi et al. A Northern Sky Survey for Point-Like Sources of EeV Neutral Particles with the Telescope Array Experiment. *Astrophys. J.*, 804(2):133, 2015. [arXiv:1407.6145](#), doi:10.1088/0004-637X/804/2/133.
 - [42] T. Abu-Zayyad et al. The Cosmic Ray Energy Spectrum Observed with the Surface Detector of the Telescope Array Experiment. *Astrophys. J.*, 768:L1, 2013. [arXiv:1205.5067](#), doi:10.1088/2041-8205/768/1/L1.
 - [43] John Matthews. Highlights from the Telescope Array Experiment. *PoS, ICRC2017:1096*, 2018. doi:10.22323/1.301.1096.
 - [44] D. Heck, J. Knapp, J. N. Capdevielle, G. Schatz, and T. Thouw. CORSIKA: A Monte Carlo code to simulate extensive air showers. 1998.
 - [45] S. Ostapchenko. QGSJET-II: Towards reliable description of very high energy hadronic interactions. *Nucl. Phys. Proc. Suppl.*, 151:143–146, 2006. [arXiv:hep-ph/0412332](#), doi:10.1016/j.nuclphysbps.2005.07.026.
 - [46] Alfredo Ferrari, Paola R. Sala, Alberto Fasso, and Johannes Ranft. FLUKA: A multi-particle transport code (Program version 2005). 2005.
 - [47] W. Ralph Nelson, H. Hirayama, and David W. O. Rogers. The Egs4 Code System. 1985.
 - [48] Piotr Homola, D. Gora, D. Heck, H. Klages, J. Pekala, M. Risse, B. Wilczynska, and H. Wilczynski. Simulation of ultrahigh energy photon propagation in the geomagnetic field. *Comput. Phys. Commun.*, 173:71, 2005. [arXiv:astro-ph/0311442](#), doi:10.1016/j.cpc.2005.07.001.
 - [49] B. T. Stokes, R. Cady, D. Ivanov, J. N. Matthews, and G. B. Thomson. Dethinning Extensive Air Shower Simulations. *Astropart. Phys.*, 35:759–766, 2012. [arXiv:1104.3182](#), doi:10.1016/j.astropartphys.2012.03.004.
 - [50] S. Agostinelli et al. GEANT4: A Simulation toolkit. *Nucl. Instrum. Meth.*, A506:250–303, 2003. doi:10.1016/S0168-9002(03)01368-8.
 - [51] T. Abu-Zayyad et al. CORSIKA Simulation of the Telescope Array Surface Detector. 2014. [arXiv:1403.0644](#).
 - [52] R.U. Abbasi et al. The bursts of high energy events observed by the telescope array surface detector. *Physics Letters A*, 381(32):2565, 2017. doi:<https://doi.org/10.1016/j.physleta.2017.06.022>.
 - [53] R. U. Abbasi et al. Gamma-ray Showers Observed at Ground Level in Coincidence With Downward Lightning Leaders. *J. Geophys. Res. Atmos.*, 123(13):6864, 2018. [arXiv:1705.06258](#), doi:10.1029/2017JD027931.
 - [54] K.L. Cummins and M. J. Murphy. An Overview of Lightning Locating Systems: History, Techniques, and Data Uses, With an In-Depth Look at the U.S. NLDN. *IEEE Trans.*, 51(3):499, 2009.
 - [55] A. Nag et al. Evaluation of U.S. National Lightning Detection Network performance characteristics using rocket-triggered lightning data acquired in 2004-2009. *J. Geophys. Res.*, 116:D02123, 2011.
 - [56] URL: <http://www.vaisala.com/en/products/thunderstormandlightningdetectionsystems/Pages/NLDN.aspx>.
 - [57] R. U. Abbasi et al. Mass composition of ultra-high-energy cosmic rays with the Telescope Array Surface Detector Data. 2018. [arXiv:1808.03680](#).
 - [58] M. Teshima et al. Properties of $10^{*}9$ -GeV - $10^{*}10$ -GeV Extensive Air Showers at Core Distances Between 100-m and 3000-m. *J. Phys.*, G12:1097, 1986. doi:10.1088/

0305-4616/12/10/017.

978-1-4613-8122-8.

- [59] J. Abraham et al. Upper limit on the diffuse flux of UHE tau neutrinos from the Pierre Auger Observatory. *Phys. Rev. Lett.*, 100:211101, 2008. [arXiv:0712.1909](#), [doi:10.1103/PhysRevLett.100.211101](#).
- [60] Grigory I. Rubtsov and Sergey V. Troitsky. Statistical methods for cosmic ray composition analysis at the Telescope Array Observatory. *J. Phys. Conf. Ser.*, 608(1):012067, 2015. [doi:10.1088/1742-6596/608/1/012067](#).
- [61] G. Ros, A. D. Supanitsky, G. A. Medina-Tanco, L. del Peral, and M. D. Rodriguez-Fras. Improving photon-hadron discrimination based on cosmic ray surface detector data. *Astropart. Phys.*, 47:10–17, 2013. [arXiv:1305.7439](#), [doi:10.1016/j.astropartphys.2013.05.014](#).
- [62] O. Deligny, K. Kawata, and P. Tinyakov. Measurement of anisotropy and the search for ultra high energy cosmic ray sources. *PTEP*, 2017(12):12A104, 2017. [arXiv:1702.07209](#), [doi:10.1093/ptep/ptx043](#).
- [63] T. Abu-Zayyad et al. Search for Anisotropy of Ultra-High Energy Cosmic Rays with the Telescope Array Experiment. *Astrophys. J.*, 757:26, 2012. [arXiv:1205.5984](#), [doi:10.1088/0004-637X/757/1/26](#).
- [64] Y. Freund and R.E. Schapire. A decision-theoretic generalization of on-line learning and an application to boosting. *Journal of Computer and System Sciences*, 55(1):119–139, 1997. [doi:10.1006/jcss.1997.1504](#).
- [65] Andreas Hocker et al. TMVA - Toolkit for Multivariate Data Analysis. *PoS, ACAT:040*, 2007. [arXiv:physics/0703039](#).
- [66] R. Brun and F. Rademakers. ROOT: An object oriented data analysis framework. *Nucl. Instrum. Meth.*, A389:81–86, 1997. [doi:10.1016/S0168-9002\(97\)00048-X](#).
- [67] Alexander Aab et al. Inferences on mass composition and tests of hadronic interactions from 0.3 to 100 EeV using the water-Cherenkov detectors of the Pierre Auger Observatory. *Phys. Rev.*, D96(12):122003, 2017. [arXiv:1710.07249](#), [doi:10.1103/PhysRevD.96.122003](#).
- [68] R. U. Abbasi et al. Depth of Ultra High Energy Cosmic Ray Induced Air Shower Maxima Measured by the Telescope Array Black Rock and Long Ridge FADC Fluorescence Detectors and Surface Array in Hybrid Mode. *Astrophys. J.*, 858(2):76, 2018. [arXiv:1801.09784](#), [doi:10.3847/1538-4357/aabad7](#).
- [69] Gary J. Feldman and Robert D. Cousins. A Unified approach to the classical statistical analysis of small signals. *Phys. Rev.*, D57:3873–3889, 1998. [arXiv:physics/9711021](#), [doi:10.1103/PhysRevD.57.3873](#).
- [70] K. M. Gorski, Eric Hivon, A. J. Banday, B. D. Wandelt, F. K. Hansen, M. Reinecke, and M. Bartelman. HEALPix - A Framework for high resolution discretization, and fast analysis of data distributed on the sphere. *Astrophys. J.*, 622:759–771, 2005. [arXiv:astro-ph/0409513](#), [doi:10.1086/427976](#).
- [71] P. Sommers. Cosmic ray anisotropy analysis with a full-sky observatory. *Astropart. Phys.*, 14:271–286, 2001. [arXiv:astro-ph/0004016](#), [doi:10.1016/S0927-6505\(00\)00130-4](#).
- [72] G. L. Cassiday et al. Mapping the UHE sky in search of point sources. *Nucl. Phys. Proc. Suppl.*, 14A:291–298, 1990. [,291(1989)]. [doi:10.1016/0920-5632\(90\)90434-V](#).
- [73] R. G. Jr. Miller. *Simultaneous Statistical Inference*. Springer-Verlag, New York, 1981. [doi:10.1007/](#)